The Astrophysical Journal Letters, 851:L2 (8pp), 2017 December 10 https://doi.org/10.3847/2041-8213/aa9c3f

Evolution of Alfvénic Fluctuations inside an Interplanetary Coronal Mass Ejection and Their Contribution to Local Plasma Heating: Joint Observations from 1.0 to 5.4 au

Hui Li[1], Chi Wang[1,2], John D. Richardson[3], and Cui Tu[4]
[1] State Key Laboratory of Space Weather, National Space Science Center, CAS, Beijing, 100190, China; hli@nssc.ac.cn
[2] University of Chinese Academy of Sciences, Beijing, 100049, China
[3] Kavli Institute for Astrophysics and Space Research, Massachusetts Institute of Technology, Cambridge, MA, USA
[4] Laboratory of Near Space Environment, National Space Science Center, CAS, Beijing, 100190, China
Received 2017 September 18; revised 2017 November 15; accepted 2017 November 21; published 2017 December 5

Abstract

Tracking an interplanetary coronal mass ejection (ICME) by widely separated spacecraft could provide us with a good opportunity to study the evolution of embedded Alfvénic fluctuations (AFs) and their possible contribution to local plasma heating directly. In this study, an ICME observed by *Wind* at 1.0 au on 1998 March 4–6 is tracked to the location of *Ulysses* at 5.4 au. AFs are commonly found inside the ICME at 1.0 au, with an occurrence rate of 21.7% and at broadband frequencies from 4×10^{-4} to 5×10^{-2} Hz. When the ICME propagates to 5.4 au, the Aflvénicity decreases significantly, and AFs are rare and only found at a few localized frequencies with the occurrence rate decreasing to 3.0%. At the same time, the magnetic strength at the AF-rich region has an extra decrease in addition to the ICME expansion effect. The energetics of the ICME are also investigated here. Under similar magnetic strength situations at 1.0 au, the turbulence cascade rate at the AF-rich region is much larger than the one at the AF-lack region. Moreover, it can be maintained during the decrease of magnetic strength if there is a lack of AFs. However, when many AFs exist, it reduces significantly as the AFs disappear. The turbulence cascade dissipation rate within the ICME is inferred to be 2688.6 J kg^{-1} s^{-1}, which satisfies the requirement of local ICME plasma heating rate, 1653.2 J kg^{-1} s^{-1}. It is therefore concluded that AF dissipation is responsible for extra magnetic dissipation and local plasma heating inside the ICME.

Key words: Sun: coronal mass ejections (CMEs) – turbulence – waves

1. Introduction

Coronal mass ejections (CMEs) are spectacular eruptions in the solar atmosphere (e.g., Kunow et al. 2006; Gopalswamy 2010). The interplanetary manifestations or the heliospheric counterparts of CMEs are referred to as Interplanetary coronal mass ejections (ICMEs; e.g., Gosling 1990), which are the key link between activities at the Sun and disturbances in the heliosphere. It is well known that ICMEs are important drivers of interplanetary shocks and disastrous space weather events, such as geomagnetic storms (e.g., Richardson & Cane 2011, and the references therein). Generally, many low-frequency magnetohydrodynamics waves, such as Alfvén waves (AWs) or Alfvénic fluctuations (AFs) and fast- and slow-mode magnetoacoustic waves, could be generated due to magnetic reconnection or catastrophe processes during the CME initiation (Kopp & Pneuman 1976; Antiochos et al. 1999; Chen & Shibata 2000). In addition, some plasma waves could also be generated by the interactions between ICMEs and the ambient solar wind.

Compared to the massive studies on the macro-structures of ICMEs, the micro-states of ICMEs, especially the wave-particle behaviors, which may contribute to particle energization and/or kinetic processes, have not been well discussed. To our best knowledge, only a few works were carried out to investigate the wave phenomena inside ICMEs. Some intense high frequency waves were found inside ICMEs, such as possible ion acoustic waves (Fainberg et al. 1996; Lin et al. 1999; Thejappa & MacDowall 2001), whistler waves, and Langmuir waves (Moullard et al. 2001). Siu-Tapia et al. (2015) recently found low-frequency waves inside eight isolated magnetic clouds based on *STEREO* observations. Zhao et al. (2017) studied 7807 electromagnetic cyclotron waves (ECWs) near the proton cyclotron frequency in and around 120 magnetic clouds during 2007–2013. For ultra-low-frequency waves, far less than the proton cyclotron frequency, some authors also discussed AWs or AFs inside ICMEs. Marsch et al. (2009) and Yao et al. (2010) found possible AF events inside two ICMEs detected by *Helios 2* at 0.7 and 0.3 au, respectively. Liang et al. (2012) later reported a clear AF event with a 1 hr duration inside an ICME at 1 au. Except for case studies, two statistical surveys have been performed to our knowledge. Li et al. (2013) investigated 27 ICMEs near 1 au, finding that AWs exist continuously for eight ICMEs, fast mode waves exist in the sheath of 13 ICMEs, and slow-mode waves exist in all events. Li et al. (2016c) extended the statistical study out to 6 au based on the 33 ICMEs observed by *Voyager 2*. They confirmed the existence of AFs inside ICMEs, and concluded that the percentage of AF duration decays linearly, in general, as ICMEs expand and move outward.

The evolution of ICMEs in the heliosphere is regarded as one of the fundamental issues in space physics. It is of great significance to study the properties and evolution characteristics of plasma waves inside ICMEs. First, the spatial distributions of AFs inside ICMEs could give some clues regarding CME initiation processes and the triggering mechanism (Liang et al. 2012). Second, the evolution and dissipation of plasma waves inside ICMEs are helpful to understand the local plasma heating (Tu & Marsch 1995; Kasper et al. 2008; Wang et al. 2014a) during the nonadiabatic expansion of ICMEs between $0.3 \sim 30$ au (Wang & Richardson 2004; Richardson et al. 2006). Liu et al. (2006) have inferred that the nonlinear cascade of low-frequency AFs caused the magnetic dissipation within ICMEs, which is sufficient to explain the in situ heating of ICME plasma. Li et al. (2016c) later found similar "W"-shaped distributions of AF occurrence and the proton temperature inside ICMEs, and confirmed the significant contribution of AFs on local ICME heating.

Among plasma waves, AWs or AFs are of interest in the present study because they are the most common wave mode in the solar wind and inside ICMEs (Bruno et al. 2006; Li et al. 2016a, 2016c). Theoretical studies suggested that the AF dissipation contributes to ICME plasma heating. Statistical observation surveys provide some indirect evidence to support such a statement. Directly tracking a specific ICME through the heliosphere by widely separated spacecraft would provide us with a good opportunity to study the evolution characteristics of embedded AFs and their contributions to ICME plasma heating, but it has never been done before. In this study, an ICME observed by *Wind* at 1 au on 1998 March 4–6 is tracked to the location of *Ulysses* at 5.4 au, and the evolution of Alfvénic fluctuations inside an ICME and their contribution to local plasma heating will be investigated in detail.

2. Evolution of Alfvénic Fluctuations inside the ICME

We analyzed data sets for the interplanetary magnetic field and solar wind plasma from both *Wind* and *Ulysses* spacecraft. For *Wind* spacecraft, the magnetic field data with a temporal cadence of 0.092 s are used from the Magnetic Field Investigation (MFI; Lepping et al. 1995), and the solar wind plasma data with a temporal cadence of 3 s are used from the three-dimensional Plasma and Energetic Particle Investigation (3DP; Lin et al. 1995). All the data from *Wind* spacecraft are in the Geocentric Solar Ecliptic (GSE) coordinates. For *Ulysses* spacecraft, the magnetic field data with a temporal resolution of 1 s are used from the Vector Helium Magnetometer (VHM; Balogh et al. 1992), and the solar wind plasma data with a temporal resolution of 4 minutes are used from the Solar Wind Observations Over the Poles of the Sun (SWOOPS; Bame et al. 1992). All the data from *Ulysses* spacecraft are in the heliographic radial tangential normal coordinate system.

The ICME was first observed by *Wind* at 1 au on 1998 March 4–6 and then passed through *Ulysses* at 5.4 au on 1998 March 23–28. During this period, these two spacecraft lined up near the ecliptic plane with the latitudinal separation of $\sim 2°$, and longitude separation of $\sim 6°$. Du et al. (2007) have confirmed that these two ICMEs are the same, with the same solar origin, by using a 1D MHD solar wind model and the Grad–Shafranov reconstruction technique. Such a great alignment between the Sun and both the spacecraft provide us with a unique opportunity to investigate the same ICME at two different evolution stages in the heliosphere. Skoug et al. (2000), Du et al. (2007), and Nakwacki et al. (2011) have studied the dynamical evolution of the magnetic cloud macrostructure from the Sun to 5.4 au by analyzing the joint observations of this ICME event.

Note that it is hard to verify that these two spacecraft passed through the same volume of plasma inside the ICME. However, this event is to our knowledge the best line-up observations of an ICEM between *Wind* and *Ulysses* spacecraft. While this is not perfect and it may have some uncertainties, it is still a good start and as good as one can hope to track the evolution of Alfvénic fluctuations inside an ICME at different radial distances. On the one hand, the corresponding CME (observed by *SOHO LASCO/C2*, 1998 February 28 12:48:00; Wang et al. 2004) of this ICME was a partial halo CME with an angular width of 169° (information from https://cdaw.gsfc.nasa.gov/CME_list/). The longitude separation is very small compared to the angular width of ICME. On the other hand, the ICME would deflect both in latitude and longitude during its radial propagation (Wang et al. 2004; Manchester et al. 2017). Based on the kinematic model of the CME deflection proposed by Isavnin et al. (2013) and Wang et al. (2014b), the ICME would deflect eastward about 9° from *Wind* to *Ulysses*. Considering that the *Ulysses* is located $\sim 6°$ east of *Wind*, such an eastward deflection of ICME would alleviate the effect of longitude separation between *Wind* and *Ulysses* spacecraft. Furthermore, the paths of both *Wind* and *Ulysses* almost intersect the center of the magnetic flux rope according to the GS reconstruction made by Du et al. (2007).

Figure 1 shows the overview of the ICME observed by *Wind* and *Ulysses*. The two vertical dashed lines represent the start and end times of the ICME, which are consistent with the results of Nakwacki et al. (2011). The shock sheath is not included here. The primary criterion of an ICME is that the proton temperature (T_p) is lower than the expected temperature ($T_{\rm ex}$) by a factor of 2. $T_{\rm ex}$ is calculated from the relationship derived by Lopez (1987). From *Wind* observations, some other ICME signatures are clear, including the enhancement of the magnetic field ($|B|$), the extreme increase of the proton number density (N_p), and the monotonic declining of solar wind bulk speed (V_p). The parameter, E_{rr} is introduced by Li et al. (2016b) to represent the goodness of the degree of the Alfvénicity, which is the mean value of the following eight parameters: (1) $||\gamma_c|-1|$; (2) $||\gamma_{cx}|-1|$; (3) $||\gamma_{cy}|-1|$; (4) $||\gamma_{cz}|-1|$; (5) $|\sigma_{\delta V}/\sigma_{\delta V_{\rm A}} - 1|$; (6) $|\sigma_{\delta V_x}/\sigma_{\delta V_{\rm Ax}} - 1|$; (7) $|\sigma_{\delta V_y}/\sigma_{\delta V_{\rm Ay}} - 1|$; and (8) $|\sigma_{\delta V_z}/\sigma_{\delta V_{\rm Az}} - 1|$. Here, the γ_c is the correlation coefficient between the fluctuations (δ) of plasma velocity ($\boldsymbol{V}$) and Alfvén velocity ($\boldsymbol{V}_{\rm A}$), and σ represents the standard deviation. The AFs are defined as the intervals with $E_{rr} \leqslant 0.3$ in this work. The time-frequency distribution of E_{rr} reveals that there exists many relatively pure AFs at broadband frequencies inside the ICME at 1 au, from 4×10^{-4} to 5×10^{-2} Hz. According to the occurrence of AFs, the ICME could be divided into two regions. The first one contains many AFs with a high degree of Alfvénicity at broadband frequencies, which is referred as the AF-rich region and represented in sky blue. The other part is a lack of AFs, which is thus called the AF-lack region and represented in pink. In general, the ICME has a duration of 30 hr with the width of 0.26 au. The average V_p, $|B|$, N_p, and T_p of the ICME at 1 au is 358.9 km s^{-1}, 11.1 nT, 11.12 cm^{-3}, and 23802 K, respectively.

When the ICME propagates to *Ulysses*, the typical ICME signatures at 1.0 au are blurred due to some interactions with the ambient solar wind. The AFs are only found at very localized frequencies. Compared to the ICME observed by *Wind* spacecraft, it has a longer duration of 107.5 hr, with the width of 0.94 au. The ICME speed has a slight increase to 364.4 km s^{-1}, while the magnetic field intensity, the number density, and the proton temperature decreases to 0.7 nT, 0.135 cm^{-3}, and 5370 K, respectively. Meanwhile, the AFs are only found at very localized frequencies, especially for the previous AF-rich region at 1 au. In addition, the magnetic field intensity at the previous AF-rich region is much less than that at the previous AF-lack region.

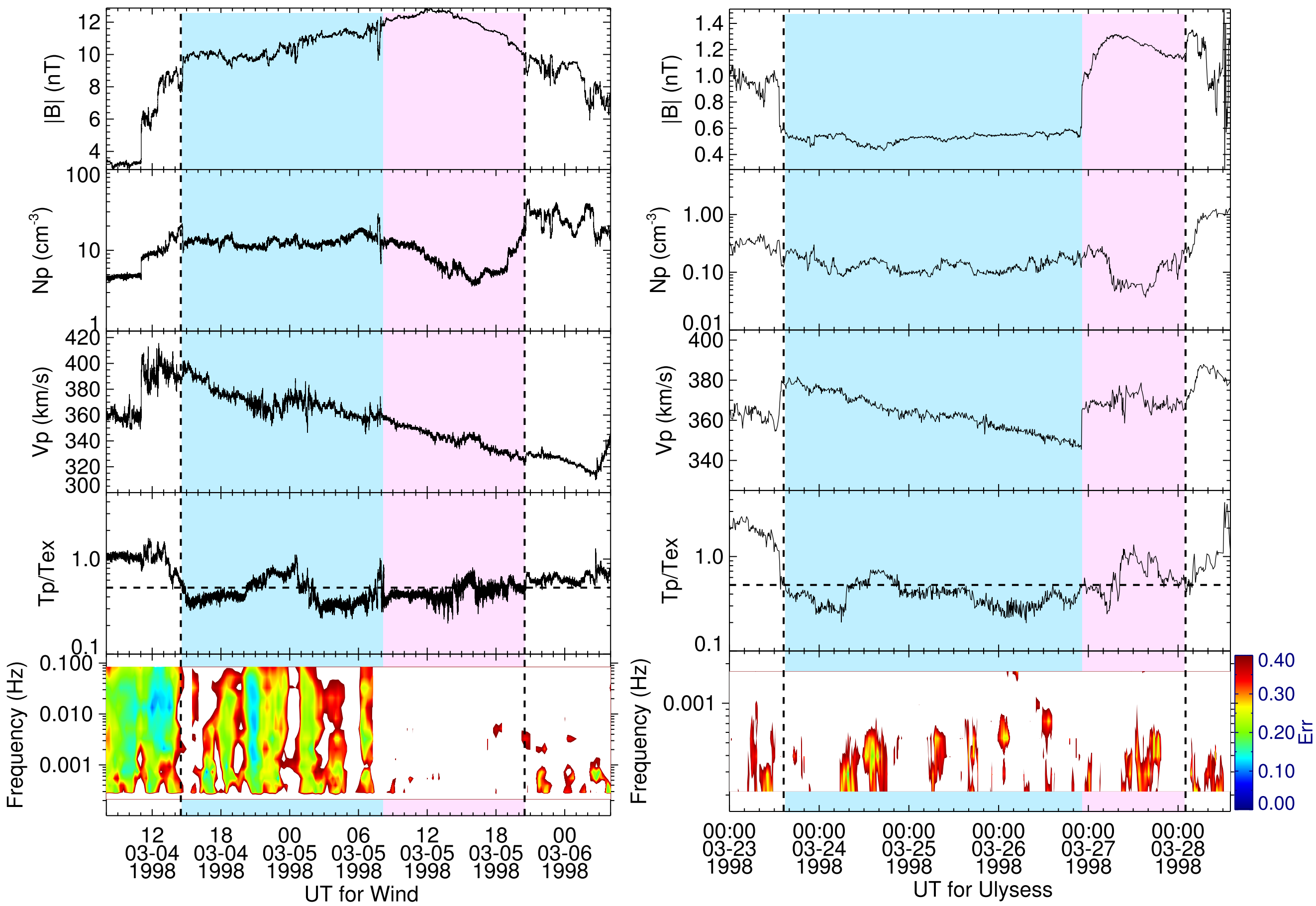

Figure 1. Overview of the ICME (between two vertical dashed lines) observed by *Wind* at 1 au and *Ulysses* at 5.4 au. From top to bottom, the panels show the magnetic field strength ($|B|$), the proton number density (N_p), the solar wind bulk speed (V_p), the ratio of the observed to the expected temperature (T_p/T_{ex}), and the parameter representing the Alfvénicity (E_{rr}), respectively. The sky blue area represents the AF-rich region, while the light pink area denotes the AF-lack region.

Figure 2 shows the distribution of relative frequency of E_{rr} inside the ICME. For the ICME observed by *Wind* at 1 au, the relative frequency of E_{rr} represents a bimodal distribution (panel (A)), with one peak at ~0.3 and the other one at ~0.6. The cumulative probability for $E_{rr} \leqslant 0.3$ is 21.7%. Panel (C) shows the comparison of relative frequency distribution of E_{rr} at the AF-rich region and at the AF-lack region. Different from the result for the whole ICME, the relative frequency distributions of E_{rr} at both the AF-rich region and the AF-lack region have a unimodal distribution, while the peak for the AF-rich region is at ~0.25 and the peak for the AF-lack region is at ~0.55. The cumulative probability for $E_{rr} \leqslant 0.3$ is 36.0% and 0.1%, respectively.

Panel (B) and (D) show the results inside the ICME observed by *Ulysses* at 5.4 au. Different from the bimodal distribution at 1.0 au, the relative frequency of E_{rr} inside the whole ICME represents a unimodal distribution with a peak at ~0.55. The cumulative probability for $E_{rr} \leqslant 0.3$ is only 3.0%. Meanwhile, the detailed distributions at both the previous AF-rich region and the AF-lack region represent a similar unimodal distribution with a peak at ~0.55. The cumulative probability for $E_{rr} \leqslant 0.3$ is 2.9% and 3.4%, respectively.

Panel (E) shows the comparison of the distribution of percentage with $E_{rr} \leqslant 0.3$ at different period bands. It is clear that the percentage of AFs with high degrees of Alfveńicity at 1.0 au is much larger than that at 5.4 au. For the ICME at 1.0 au, the percentages are more than 20% with the period band from 30 s to 4000 s. However, those percentages are nearly 1% with the period band from 500 to 1000 s and are less than 8% with the period band from 2000 to 5000 s. The contribution of AF dissipation from 1.0 to 5.4 au to the evolution of ICME energetics will be discussed in the next section.

3. Energetics Analysis of the ICME

The magnetic fluctuations inside an ICME represented a power spectrum in the form of $f^{-5/3}$ at spacecraft-frame frequencies less than 0.5 Hz (Leamon et al. 1998). Based on the Kolmogoroff's theory, such an inertial range spectrum indicates strong spectral energy transfer. The turbulence cascade rate ($\varepsilon_{\mathrm{ko}}$) can be deduced from the Kolmogoroff spectrum (Coleman 1968; Leamon et al. 1999; Liu et al. 2006). Vasquez et al. (2007) later made some corrections for the coefficients and the expression is as follows

$$\varepsilon_{\mathrm{ko}} = \frac{\alpha_1 + \sqrt{\alpha_1}}{2}\left(\frac{2}{1+\alpha_1}\right)^{3/2}\frac{2\pi}{V_{\mathrm{SW}}}\left[\frac{5(1+R_A)}{3C_{\mathrm{ko}}}\right]^{3/2} \times f^{5/2}\left[\frac{P(f)}{\mu_0 m_p N_p}\right]^{3/2}, \tag{1}$$

where C_{ko} is a numerical constant, which is assumed to be 1.6 here (Sreenivasan 1995; Yeung & Zhou 1997). V_{SW} is the solar wind bulk speed. $P[f]$ is the observed frequency spectrum of magnetic fluctuations in the inertial range. m_p is the proton

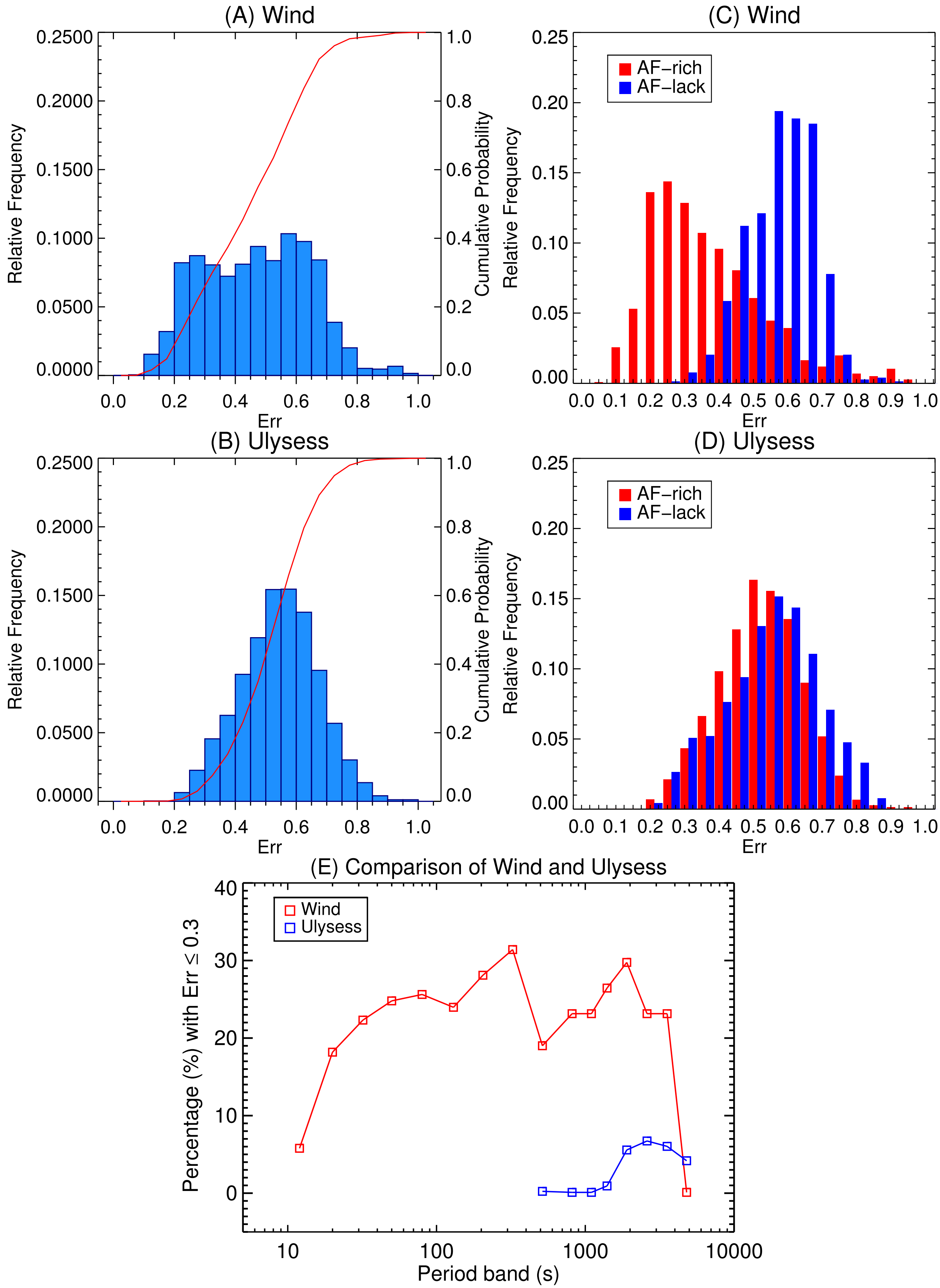

Figure 2. Distribution of relative frequency of E_{rr} inside the whole ICME: (A) *Wind*; (B) *Ulysses*. The red line represents the cumulative probability. Comparison of relative frequency distribution of E_{rr} at the AF-rich region and at the AF-lack region: (C) *Wind*; (D) *Ulysses*. Comparison of the distribution of percentage with $E_{rr} \leqslant 0.3$ at different period bands are shown in panel (E).

mass. R_A is the ratio between kinetic energy and magnetic energy; α_1 is the Elsässer ratio, which is $= (1-\sigma_c)/(1+\sigma_c)$; σ_c is the normalized cross-helicity (Tu & Marsch 1995). Here, we will follow the approach carried out by Leamon et al. (1999) and Liu et al. (2006) to determine the turbulence dissipation rate inside the ICME.

Figure 3 shows the power spectral density of magnetic fluctuations inside the ICME. The power-law fittings are done for both the inertial range (red dashed lines) and the dissipation range (green dashed lines). The left three panels are for the ICME observed by *Wind* at 1.0 au. The power spectra show significant steepening at high frequencies, which marks the onset of magnetic dissipation (Leamon et al. 1999). For the whole ICME, the power spectra "break" from a $f^{-1.65}$ power law in the inertial range to a $f^{-2.54}$ power law in the dissipation range. The spectral index in the inertial range is in good agreement with the Kolmogoroff prediction of $5/3$ and the statistical results of 1.56 obtained by Smith et al. (2006), while the spectral index in the dissipation range is a little larger than the average value of 2.01 obtained by Smith et al. (2006). For the AF-rich and AF-lack regions, the spectral indexes in the inertial range are 1.63 and 1.66, respectively; meanwhile, the spectral indexes in the dissipation range are 2.63 and 1.93, respectively, indicating that the spectral cascade in the AF-rich region tends to be higher than that in the AF-lack region (Smith et al. 2006). The break frequency, f_b, is $0.3 \sim 0.5$ Hz, comparable to but less than the frequency corresponding to the ion inertial length, $f_{di} = V_{\rm SW}/(2\pi d_i)$, which is $0.7 \sim 0.9$ Hz, where d_i is the ion inertial length. The proton gyro-frequency, $f_{\rm pc}$, is about 0.2 Hz. The frequencies corresponding to some other scales (see Table 2 in Chen et al. 2014), such as ρ_i, the ion gyro-radius, ρ_s, the ion sound gyro-radius, $(d_i^{-2} + \rho_s^{-2})^{-1/2}$, and $di + \rho_i$, have also been calculated but not shown here. Among these frequencies, f_{di} is the most close to f_b. Considering the ion beta value during this ICME is much less than 1, $0.04 \sim 0.11$, our results are in agreement with the conclusion of Chen et al. (2014). The right three panels are for the ICME observed by *Ulysses* at 5.4 au. The power spectra for the whole ICME, the previous AF-rich and AF-lack region, nearly obey the Kolmogoroff's theory, with the spectral indexes in the inertial range of 1.58, 1.60, and 1.57, respectively. However, the power spectra have flattened in the dissipation range for the whole ICME and the previous AF-rich region, with the spectral indexes of 1.12 and 0.82, respectively, which may be aliased by the instrument noises. The power spectrum for the previous AF-lack region still has a steepening in the dissipation range, with the spectral index of 1.84. Similarly, the break frequencies are also comparable to the frequency corresponding to the ion inertial length.

The energy cascade rate then can be calculated from Equation (1). For the whole ICME, the energy cascade rates at 1.0 au are derived to be about 2688.6 J kg^{-1} s^{-1}, which is close to the lower limit ($2970 \sim 65{,}320$) estimated by Vasquez et al. (2007) when the solar wind speed is between 350 and 400 km s^{-1}. When the ICME propagates to 5.4 au, this value reduces to 274.7 J kg^{-1} s^{-1}, suggesting that the capacity of turbulence cascade reduces as the ICME propagates outward. For the AF-rich region, the energy cascade rate drops from 3312.2 to 89.7 J kg^{-1} s^{-1} accompanied with the disappearance of AFs, when the ICME propagates from *Wind* to *Ulysses*. For comparison, the energy cascade rates for the AF-lack region can be maintained at a certain level, and the values at 1.0 and 5.4 au are 526.9 and 737.3 J kg^{-1} s^{-1}, respectively. In addition, Smith et al. (2006) have found the dependence of the dissipation range spectrum on the rate of energy cascade through the inertial range. Our results are also in agreement with their findings that the steeper spectral in the dissipation range forms from greater cascade rates.

Liu et al. (2006) have taken into account the Coulomb energy transfer between protons and alphas, and derived the equations of the heating rate required for protons (ε_p) and alphas (ε_α) to produce the observed temperature profile. The specific expressions are as follows

$$\varepsilon_p = \frac{k_{\rm B} T_p}{m_p}\left[\frac{3V_{\rm SW}}{2}\frac{d}{dr}\ln T_p - \frac{3\left(\frac{T_\alpha}{T_p} - 1\right)}{2\tau_{p\alpha}} + \frac{1}{\tau_e}\right] \qquad (2)$$

$$\varepsilon_\alpha = \frac{k_{\rm B} T_\alpha}{m_\alpha}\left[\frac{3V_{\rm SW}}{2}\frac{d}{dr}\ln T_\alpha - \frac{3\left(\frac{T_p}{T_\alpha} - 1\right)}{2\tau_{\alpha p}} + \frac{1}{\tau_e}\right], \qquad (3)$$

where $k_{\rm B}$ is the Boltzmann constant, T_p and T_α are the temperature of protons and alphas, m_α is the alpha mass, $\tau_{p\alpha}$ and $\tau_{\alpha p}$ are the Coulomb collision timescales and have a relationship of $\frac{\tau_{\alpha p}}{\tau_{p\alpha}} = \frac{n_\alpha}{n_p}$, n_α is the alpha number density, and τ_e is the expansion time of the plasma. For more details, please refer to Appendix A in Liu et al. (2006). The total required heating rate ($\varepsilon_{\rm re}$) is then obtained as

$$\varepsilon_{re} = \varepsilon_p + \varepsilon_\alpha. \qquad (4)$$

Based on the observations at 1.0 and 5.4 au, we can quantitatively estimate the required heating rate, $\varepsilon_{\rm re}$, to be about 1653.2 J kg^{-1} s^{-1}, which is larger than the upper limit ($325 \sim 1234$) estimated by Vasquez et al. (2007), and is less than the average estimation of 2550 made by Liu et al. (2006), but is consistent with the result of 1600 given by Smith et al. (2001). At the same time, the turbulence cascade rate inside the whole ICME at 1.0 au, 2688.6 J kg^{-1} s^{-1}, can satisfy such a heating requirement.

4. Comparison of the AF-rich Region and AF-lack Region

Table 1 gives a summary of some properties of the ICME observed at 1.0 and 5.4 au. From 1.0 to 5.4 au, the occurrence rate of AFs in the AF-lack region are both very rare, about 0.1% and 3.4%. However, for the AF-rich region, the AF occurrence rate significantly deceases from 36% to 2.9%, indicating an almost total disappearance of AFs.

One consequence of AF disappearance through dissipation is an extra magnetic field intensity attenuation. The width of the ICME, estimated from ICME duration and propagating speed, increases from 0.26 to 0.94 au, about 3.6 times. Accordingly, the area of the ICME cross section increases by nearly 13.1 times in the hypothesis of the circular cross section. Considering the conservation of magnetic flux, the magnetic field strength should have an about 13.1 times decrease. For the AF-lack region, the magnetic field intensity changes from 11.9 to 1.19 nT, 10 times, which satisfies the conservation of magnetic flux. However, for the AF-rich region, the magnetic field intensity changes from 10.5 to 0.53 nT by 19.8 times, which is much larger than expected, indicating the existence of an extra magnetic field strength depression.

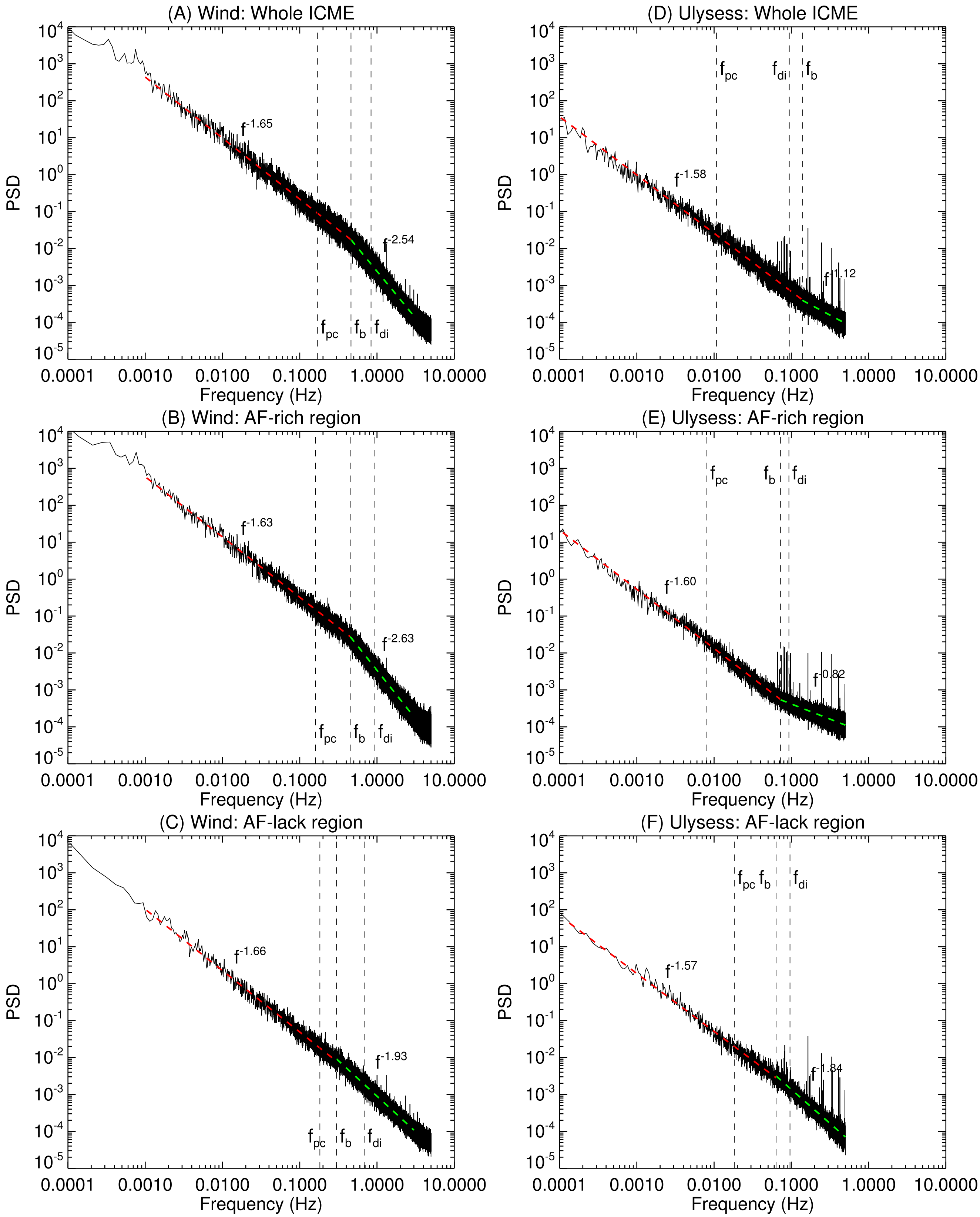

Figure 3. Power spectral density of magnetic fluctuations inside the ICME: (A) the whole ICME observed by *Wind* at 1.0 au; (B) the AF-rich region of the ICME at 1.0 au; (C) the AF-lack region of the ICME at 1.0 au; (D) the whole ICME observed by *Ulysses* at 5.4 au; (B) the AF-rich region of the ICME at 5.4 au; (C) the AF-lack region of the ICME at 5.4 au. The dashed colored lines are the power-law fitting results. The red ones are in the inertial range, while the green ones are in the dissipation range. The vertical dashed lines represent the proton gyro-frequency, f_{pc}, the break frequency, f_b, and the frequency corresponding to the ion inertial length, f_{di}.

Table 1
A Summary of Some Properties of the ICME Observed at 1.0 and 5.4 au

	Wind		*Ulysses*	
	AF-rich Region	AF-lack Region	AF-rich Region	AF-lack Region
Width (au)	0.26		0.94	
AF occurrence	36%	0.1%	2.9%	3.4%
$\|B\|$ (nT)	10.5	11.9	0.53	1.19
$\varepsilon_{\rm ko}$ (J kg^{-1} s^{-1})	3312.2	526.9	89.7	737.3
$\varepsilon_{\rm re}$ (J kg^{-1} s^{-1})	1653.2			

The other consequence of AF disappearance is the reduction of the turbulence cascade rate. At 1.0 au, the turbulence cascade rate at the AF-rich region is 6.3 times larger than that at the AF-lack region because of the existence of AFs. With the disappearance of AFs at the AF-rich region from 1.0 to 5.4 au, the turbulence cascade rate decays significantly from 3312.2 to 89.7 J kg^{-1} s^{-1}, about 36.9 times. However, the turbulence cascade rates at the AF-lack region can maintain a certain level, indicating such an extreme decrease is not simply caused by the normal depression of magnetic filed intensity. AF dissipation should play a key role in the energy transfer. In addition, the required heating rate is estimated to be 1653.2 J kg^{-1} s^{-1}, indicating that the turbulence cascade rate is enough to supply the required heating rate.

5. Summary

In this study, we track an ICME from 1.0 to 5.4 au using the data from *Wind* and *Ulysses* spacecraft. Such an event provides us with a good opportunity to study the evolution of embedded AFs within an ICME and their contributions to local plasma heating directly. The ICME at 1.0 au could be divided into two regions according to the occurrence of AFs. The first one contains many AFs with high degrees of Aflvénicity at broadband frequencies from 4×10^{-4} to 5×10^{-2} Hz, which is referred to as the AF-rich region. The other part is a lack of AFs, which is thus called the AF-lack region. When the ICME propagates to 5.4 au, the Aflvénicity decreases significantly and the AFs at the AF-rich region are only found at a few localized frequencies. The occurrence rate of AFs inside ICME at 5.4 au decreases to 3.0% from 21.7% at 1.0 au. Because of the ICME expansion effect, the magnetic field intensity has decreased by 10.0 times for the AF-lack region. However, it decreases by 19.8 times for the AF-rich region, indicating the existence of an extra magnetic dissipation.

We estimate the energetics of the ICME at different radial distances. The turbulence cascade rate is estimated from the inertial range power spectrum of magnetic fluctuations, and the required heating rate is derived from the approach proposed by Vasquez et al. (2007). Under a similar magnetic field intensity situation at 1.0 au, the turbulence cascade rate within the AF-rich region is much larger than the value within the AF-lack region, 3312.3 versus 526.9 J kg^{-1} s^{-1}. As the ICME propagates to 5.4 au, the turbulence cascade rate for the previous AF-rich region significantly drops to 89.7 J kg^{-1} s^{-1} by 36.9 times accompanied with the disappearance of AFs. However, for the previous AF-lack region, it can maintain a certain level to 737.3 J kg^{-1} s^{-1} in spite of a corresponding 10 times decrease of magnetic field intensity. The turbulence cascade dissipation rate within the whole ICME at 1.0 au is inferred to be 2688.6 J kg^{-1} s^{-1}, which satisfies the requirement of the local ICME plasma heating rate, 1653.2 J kg^{-1} s^{-1}.

Based on the above results, the AFs inside ICMEs are believed to be important to the dynamic evolution of ICMEs. They are suggested to be responsible for the extra depression of magnetic strength depression and the reduction of the capacity of turbulence cascade as the ICME propagates outward. The decrease of magnetic energy thus contributes to the local plasma heating inside the ICME.

We thank the *Wind* and *Ulysses* Mission for the use of their data. The data are accessible at the NSSDC (ftp://nssdcftp.gsfc.nasa.gov). We also thank Dr. J. S. He from Peking University and Dr. X. Wang from Beijing University of Aeronautics and Astronautics for many valuable discussions. This work was supported by NNSFC grants 41574169 and 41731070 and Young Elite Scientists Sponsorship Program by CAST, 2016QNRC001. H.L. was also supported by Youth Innovation Promotion Association of the Chinese Academy of Sciences and in part by the Specialized Research Fund for State Key Laboratories of China.

ORCID iDs

Hui Li https://orcid.org/0000-0002-4839-4614
John D. Richardson https://orcid.org/0000-0003-4041-7540

References

Antiochos, S. K., Devore, C. R., & Klimchuk, J. A. 1999, ApJ, 510, 485
Balogh, A., Beek, T. J., Forsyth, R. J., et al. 1992, A&AS, 92, 221
Bame, S. J., McComas, D. J., Barraclough, B. L., et al. 1992, A&AS, 92, 237
Bruno, R., Bavassano, B., D'Amicis, R., et al. 2006, SSRv, 122, 321
Chen, C. H. K., Leung, L., Boldyrev, S., et al. 2014, GeoRL, 41, 8081
Chen, P., & Shibata, K. 2000, ApJ, 545, 524
Coleman, P. J., Jr 1968, ApJ, 153, 371
Du, D., Wang, C., & Hu, Q. 2007, JGR, 112, A09101
Fainberg, J., Osherovich, V. A., Stone, R. G., MacDowall, R. J., & Balogh, A. 1996, in AIP Conf. Proc. 382, Solar Wind 8, ed. D. Winterhalter et al. (Melville, NY: AIP), 554
Gopalswamy, N. 2010, in Proc. 20th National Solar Physics Meeting, ed. I. Dorotovic (Hurbanovo: Slovak Central Observatory), 108
Gosling, J. T. 1990, GMS, 58, 343
Isavnin, A., Vourlidas, A., & Kilpua, E. K. J. 2013, SoPh, 284, 203
Kasper, J. C., Lazarus, A. J., & Gary, S. P. 2008, PhRvL, 101, 261103
Kopp, R. A., & Pneuman, G. W. 1976, SoPh, 50, 85
Kunow, H., Crooker, N. U., Linker, J. A., Schwenn, R., & Von Steiger, R. 2006, Coronal Mass Ejections (Dordrecht: Springer)
Leamon, R. J., Smith, C. W., & Ness, N. F. 1998, GeoRL, 25, 2505
Leamon, R. J., Smith, C. W., Ness, N. F., & Wong, H. K. 1999, JGR, 104, 22331
Lepping, R. P., Acũna, M. H., Burlaga, L. F., et al. 1995, SSRv, 71, 207
Li, H., Wang, C., Belcher, J. W., He, J. S., & Richardson, J. D. 2016a, ApJL, 824, L2
Li, H., Wang, C., Chao, J. K., & Hsieh, W. C. 2016b, JGR, 121, 42
Li, H., Wang, C., He, J., et al. 2016c, ApJL, 831, L13
Li, Q., Xiao, C., Wang, H., Chen, Y., & Wang, X. 2013, SSPMA, 43, 1306
Liang, H., Xiao, C., Zhou, G., et al. 2012, PlST, 14, 102
Lin, N., Kellogg, P. J., Goetz, K. A., Monson, S. J., & MacDowall, R. J. 1999, in AIP Conf. Proc. 471, Solar Wind 9, ed. S. T. Suess, G. A. Gary, & S. F. Nerney (Melville, NY: AIP), 673
Lin, R. P., Anderson, K. A., Ashford, S., et al. 1995, SSRv, 71, 125
Liu, Y., Richardson, J. D., Belcher, J. W., & Kasper, J. C. 2006, JGR, 111, A01102
Lopez, R. E. 1987, JGR, 92, 11189
Manchester, W., Kilpua, E. K. J., Liu, Y. D., et al. 2017, SSRv, 212, 1159
Marsch, E., Yao, S., & Tu, C.-Y. 2009, AnGeo, 27, 869
Moullard, O., Burgess, D., Salem, C., et al. 2001, JGR, 106, 8301
Nakwacki, M. S., Dasso, S., Démoulin, P., Mandrini, C. H., & Gulisano, A. M. 2011, A&A, 535, A52
Richardson, I. G., & Cane, H. V. 2011, SpWea, 9, S07005

Richardson, J. D., Liu, Y., Wang, C., & Burlaga, L. F. 2006, AdSpR, 38, 528
Siu-Tapia, A., Blanco-Cano, X., Kajdic, P., et al. 2015, JGR, 120, 2363
Skoug, R. M., Feldman, W. C., Gosling, J. T., et al. 2000, JGR, 105, 27269
Smith, C. W., Isenberg, P. A., Matthaeus, W. H., & Richardson, J. D. 2006, ApJ, 638, 508
Smith, C. W., Matthaeus, W. H., Zank, G. P., et al. 2001, JGR, 106, 8253
Sreenivasan, K. R. 1995, PhFl, 7, 2778
Thejappa, G., & MacDowall, R. J. 2001, in The 3D Heliosphere at Solar Maximum, ed. R. G. Marsden (Dordrecht: Springer), 211
Tu, C.-Y., & Marsch, E. 1995, SSRv, 73, 1
Vasquez, B. J., Smith, C. W., Hamilton, K., et al. 2007, JGR, 112, A07101
Wang, C., & Richardson, J. D. 2004, JGR, 109, A06104
Wang, C. B., Wang, B., & Lee, L. C. 2014a, SoPh, 289, 3895
Wang, Y., Shen, C., Wang, S., et al. 2004, SoPh, 222, 329
Wang, Y., Wang, B., Shen, C., et al. 2014b, JGR, 119, 5117
Yao, S., Marsch, E., Tu, C.-Y., & Schwenn, R. 2010, JGR, 115, A05103
Yeung, P. K., & Zhou, Y. 1997, PhRvE, 56, 1746
Zhao, G. Q., Chu, Y. H., Lin, P. H., et al. 2017, JGR, 122, 4879